Supporting Information for

Interfacing Soft and Hard Materials with Triple-Shape-Memory and Self-Healing Functions

Aslihan Argun[1], Umit Gulyuz[1,2], and Oguz Okay *[1]

[1]Istanbul Technical University, Department of Chemistry, 34469 Maslak, Istanbul, Turkey,
[2]Kirklareli University, Department of Chemistry and Chemical Processing Technologies, 39750 Luleburgaz, Kirklareli, Turkey

Table of Contents

Requirements for preparing mechanical strong hybrid hydrogels

Preliminary experiments highlighted two requirements for preparing mechanical strong hybrid hydrogels with smooth and robust interfaces:

(i) Swelling ratios of the gel components of hybrids should not differ significantly from each other. Otherwise, they easily rupture in aqueous environment. For instance, hybrids consisting of loosely and highly covalently cross-linked polyacrylamide,[1] poly(acrylic acid),[2] or pol(dimethylacrylamide) hydrogels,[3] acting as the soft and hard components, respectively, were prepared via the limited diffusion approach of the monomer solutions. Because the degree of swelling depends on the cross-link density,[1-3] the mismatch in the swelling ratios of the gel components induced a swelling pressure from the loosely-cross-linked soft to the highly cross-linked hard zones resulted in breaking of hybrids when immersed in water.

(ii) The interface region in hybrids should be stronger than its components and this region should exhibit a smooth transition in the mechanical performance from one to another zone. This is the most critical condition because hard-soft interfaces with large differences in the mechanical properties are subject to increased chances of failure.[4-6] For instance, photopolymerization of methacrylated hyaluronic acid (GMHA) in water, as described in ref.[7] produced a suitable soft gel for biomedical applications. However, during the preparation of hybrids, no significant diffusion of the second solution of the monomers such as DMA to the viscous GMHA solution occurred resulted in a weak interface that easily ruptured under strain.

References

(1) Orakdogen, N.; Okay, O. Correlation between crosslinking efficiency and spatial inhomogeneity in poly(acrylamide)hydrogels. Polym. Bull. 2006, 57, 631-641.

(2) Yazici, I.; Okay, O. Spatial inhomogeneity in poly(acrylic acid) hydrogels. Polymer 2005, 46, 2595-2602.

(3) Gundogan, N.; Okay, O.; Oppermann, W. Swelling, elasticity and spatial inhomogeneity of poly(N,N-dimethylacrylamide) hydrogels formed at various polymer concentrations. Macromol. Chem. Phys. 2004, 205, 814-823.

(4) Genin, G.M.; Kent, A.; Birman, V.; Wopenka, B.; Pasteris, J.D.; Marquez, P.J.; Thomopoulos, S. Functional grading of mineral and collagen in the attachment of tendon to bone. *Biophys. J.* **2009**, 97, 976–985.

(5) Wren, T.A.L.; Yerby, S.A.; Beaupré, G.S.; Carter, R.R. Mechanical properties of the human achilles tendon. *Clin. Biomech.,* **2001**, 16, 245-251.

(6) Thomopoulos, S.; Birman, V.; Genin, G.M. in *Structural Interfaces and Attachments in Biology*. (Eds.: Thomopoulos, S.; Birman, V.; Genin, G.M.) 3-17, **2013**, Springer.

(7) Tavsanli, B.; Can, V.; Okay, O. Mechanically strong triple network hydrogels based on hyaluronan and poly(N,N-dimethylacrylamide). *Soft Matter* **2015**, 11, 8517-8524.

Table S1: Compressive mechanical properties of the gel components, mixture gels, and hybrids.

Code	Composition (mol%)				24 °C			37 °C		
	DMA	**C18A**	**C17.3M**	**C12M**	***E* / MPa**	**ε_f %**	**σ_f / MPa**	***E* / MPa**	**ε_f %**	**σ_f / MPa**
C1	70	30	-	-	54 (7)	80 (3)	59 (15)	27 (4)	84 (2)	50 (11)
C2	50	-	50	-	62(7)	85 (1)	56 (8)	0.34 (0.04)	93 (0)	30 (3)
C3	50	-	-	50	0.27 (0.03)	93 (1)	34 (4)	-	-	-
C1+C2	60	15	25	-	102 (13)	82 (0)	71 (11)	61 (6)	85 (2)	60 (10)
C1+C3	60	15	-	25	0.45 (0.03)	93.4 (0.4)	16 (3)	-	-	-
C1/C2	varies at the interface				47 (6)	76 (6)	30 (4)	15 (1)	84 (2)	27 (4)
C1/C3	varies at the interface				32 (5)	83 (1)	24 (3)	-	-	-

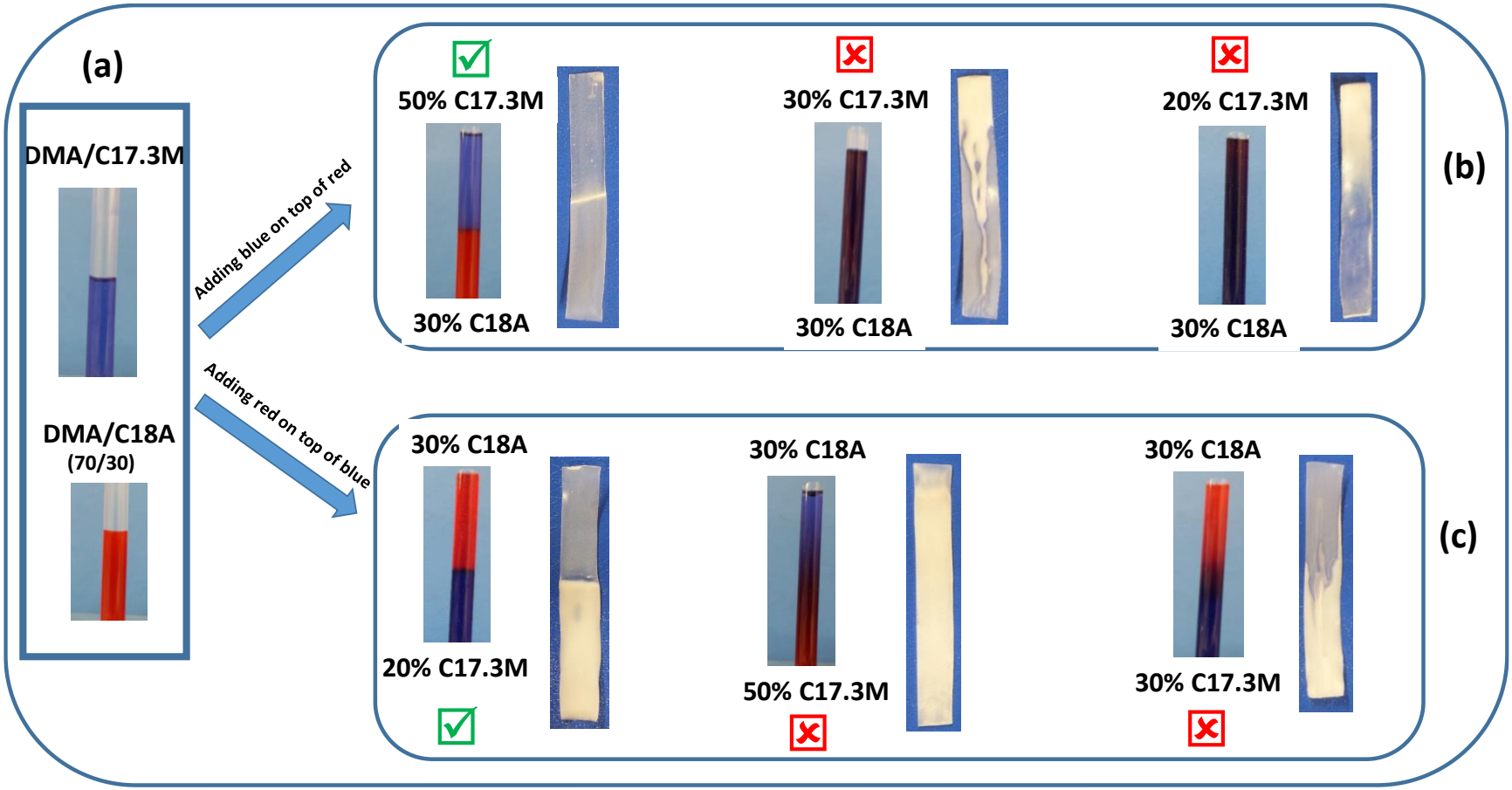

Figure S1. (a): Images of DMA/C17.3M and DMA/C18A monomer mixtures colored with blue and red, respectively. **(b, c)**: Images of solutions and resulting hybrid hydrogels after addition of DMA/C17.3M at various compositions on top of DMA /C18A at a molar ratio of 70/30 (b) and vice versa (c).

Hydrophobic monomer content (in mol%) of the monomer mixture	Density (g/mL)	Images of solutions and gels
50% C17.3M (blue)	0.881	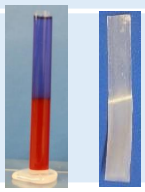
30% C18A (red)	0.894	
30% C17.3M (blue)	0.895	
30% C18A (red)	0.894	
20% C17.3M (blue)	0.912	
30% C18A (red)	0.894	

Hydrophobic monomer content (in mol%) of the monomer mixture	density (g/mL)	Images of solutions and gels
30% C18A (red)	0.894	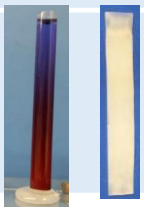
50% C17.3M (blue)	0.881	
30% C18A (red)	0.894	
30% C17.3M (blue)	0.895	
30% C18A (red)	0.894	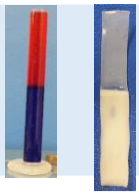
20% C17.3M (blue)	0.912	

(a)

50% C12M (blue)	0.889	
30% C18A (red)	0.894	
30% C12M (blue)	0.907	
30% C18A (red)	0.894	
20% C12M (blue)	0.921	
30% C18A (red)	0.894	

30% C18A (red)	0.894	
50% C12M (blue)	0.889	
30% C18A (red)	0.894	
30% C12M (blue)	0.907	
30% C18A (red)	0.894	
20% C12M (blue)	0.921	

(b)

Hydrophobic monomer content (in mol%) of the monomer mixture	Density (g/mL)	Images of solutions and gels
50% C17.3M (blue)	0.881	
50% C18A (red)	0.881	
30% C17.3M (blue)	0.895	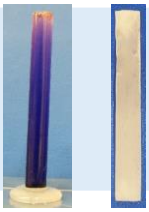
50% C18A (red)	0.881	
20% C17.3M (blue)	0.912	
50% C18A (red)	0.881	

Hydrophobic monomer content (in mol%) of the monomer mixture	Density (g/mL)	Images of solutions and gels
30% C18A (red)	0.881	
50% C17.3M (blue)	0.881	
30% C18A (red)	0.881	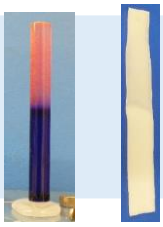
30% C17.3M (blue)	0.895	
30% C18A (red)	0.881	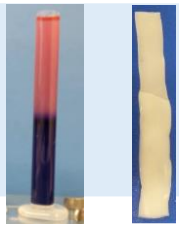
20% C17.3M (blue)	0.912	

(c)

50% C12M (blue)	0.889	
50% C18A (red)	0.881	
30% C12M (blue)	0.907	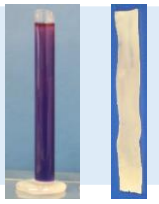
50% C18A (red)	0.881	
20% C12M (blue)	0.921	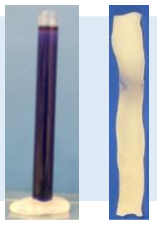
50% C18A (red)	0.881	

50% C18A (red)	0.881	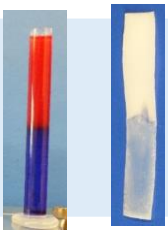
50% C12M (blue)	0.889	
50% C18A (red)	0.881	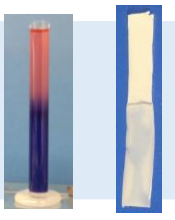
30% C12M (blue)	0.907	
50% C18A (red)	0.881	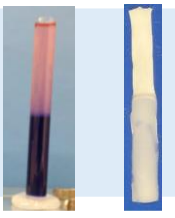
20% C12M (blue)	0.921	

(d)

Figure S2. Images of DMA/hydrophobic monomer mixtures of various compositions and the resulting hybrid hydrogels after addition one mixture on top of the other mixture. Hydrophobic monomer content of the mixtures and their densities are shown.

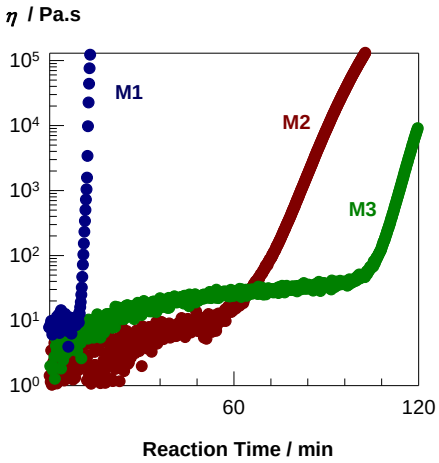

Figure S3. Viscosity of M1, M2, and M3 monomer mixtures during UV-initiated polymerization at 25 °C plotted against the reaction time.

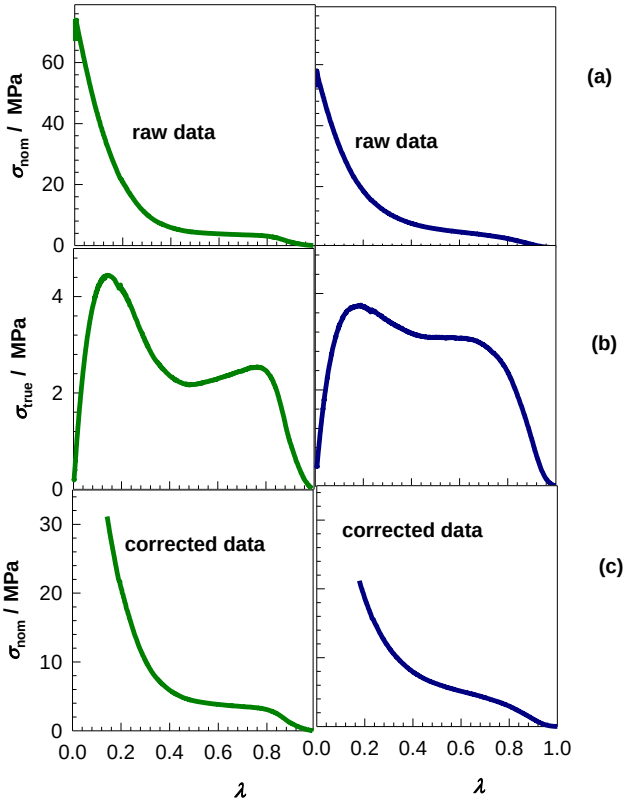

Figure S4. Typical compressive stress-strain curves of hybrid hydrogels as the dependences of σ_{nom} and σ_{true} on the strain λ. One of the gel components is obtained from DMA/C18A monomer mixture at a molar ratio of 70/30. The other component is from DMA/C17.3M monomer mixture at a molar ratio of 50/50 (left panel) and 70/30 (right panel). The bottom panel shows the corrected nominal stress – strain curves up the maximum strain in σ_{true}–λ plots.

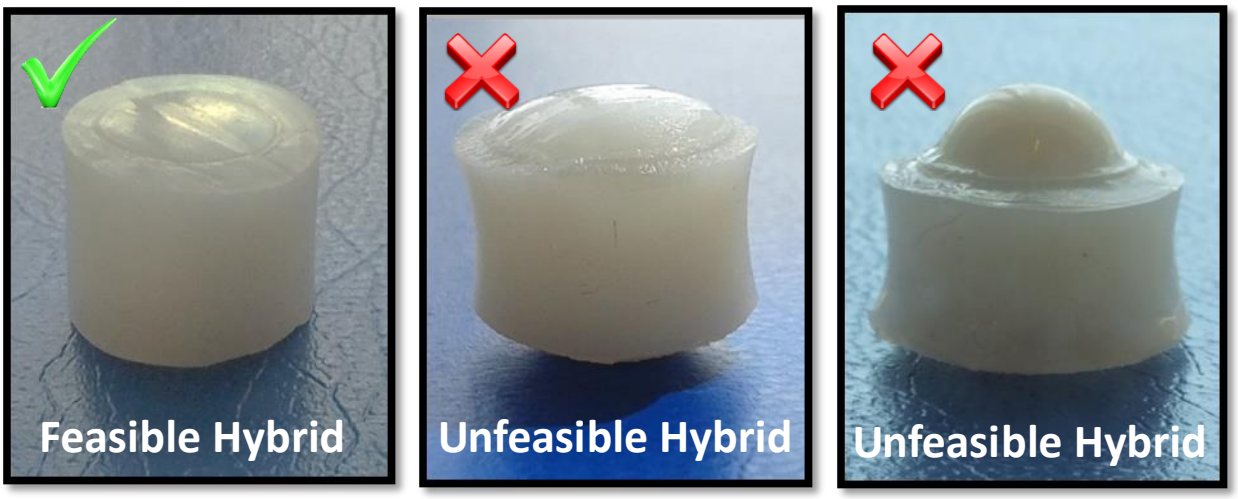

Figure S5. Images of cylindrical hybrid gel specimens consisting of C3 core formed using 50, 20, and 10 mol% C12M (from left to right) surrounded by the C1 outer layer. Decreasing C12M content of the core increases its swelling ratio in water resulting in an easier rupture in aqueous environment.

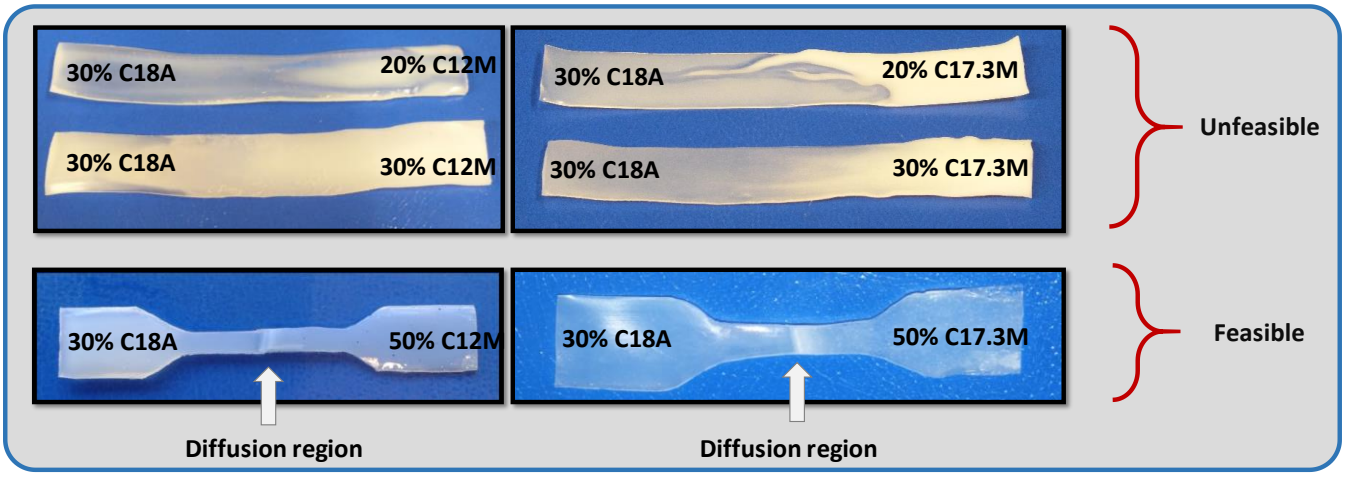

Figure S6. Images of hybrid hydrogels composed of gel components consisting of poly(DMA) chains containing hydrophobic C18A and C12M units. The amount of C18A was fixed at 30 mol% while the amount of C12M was varied between 20 and 50 mol %.

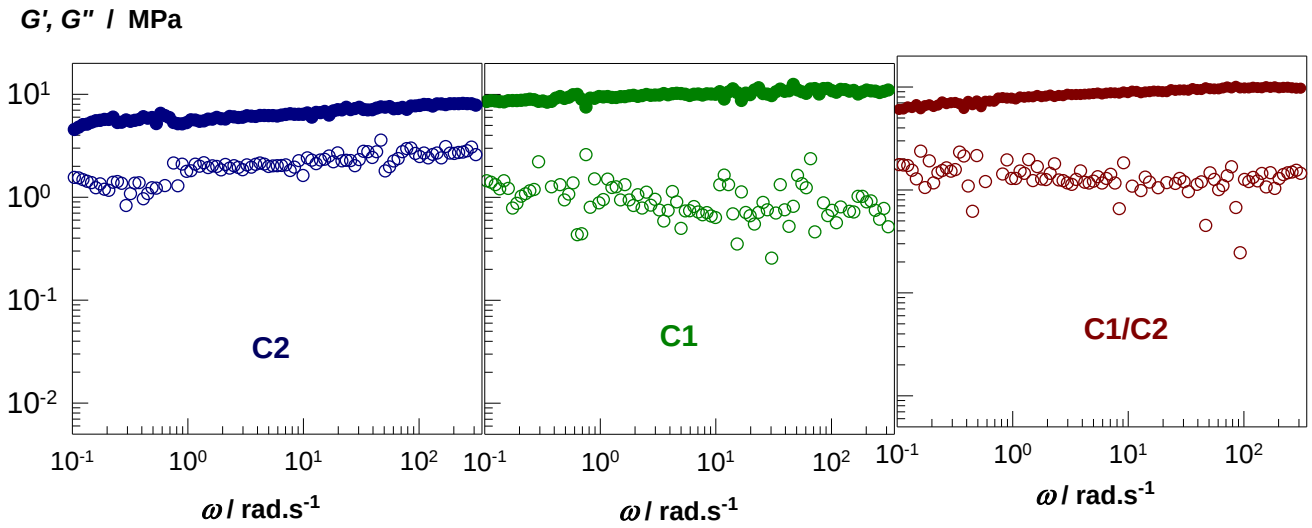

Figure S7. Frequency dependences of *G'* (filled symbols) and *G''* (open symbols) of C2, C1, and C1/C2 hydrogels at 25 °C. γ_0 = 0.1%.